PNAS RESEARCH ARTICLE | CHEMISTRY

Silica particles convert thiol-containing molecules to disulfides

Yangjie Li[a,1], Kurt W. Kolasinski[b], and Richard N. Zare[a,1]

Edited by Laura Gagliardi, The University of Chicago, Chicago, IL; received March 25, 2023; accepted July 14, 2023

Synthetic amorphous silica is a common food additive and a popular cosmetic ingredient. Mesoporous silica particles are also widely studied for their potential use in drug delivery and imaging applications because of their unique properties, such as tunable pore sizes, large surfaces areas, and assumed biocompatibility. Such a nanomaterial, when consisting of pure silicon dioxide, is generally considered to be chemically inert, but in this study, we showed that oxidation yields for different compounds were facilitated by simply incubating aqueous solutions with pure silica particles. Three thiol-containing molecules, L-cysteine, glutathione, and D-penicillamine, were studied separately, and it was found that more than 95% of oxidation happened after incubating any of these compounds with mesoporous silica particles in the dark for a day at room temperature. Oxidation increased over incubation time, and more oxidation was found for particles having larger surface areas. For nonporous silica particles at submicron ranges, yields of oxidation were different based on the structures of molecules, correlating with steric hindrance while accessing surfaces. We propose that the silyloxy radical (SiO•) on silica surfaces is what facilitates oxidation. Density functional theory calculations were conducted for total energy changes for reactions between different aqueous species and silicon dioxide surfaces. These calculations identified two most plausible pathways of the lowest energy to generate SiO• radicals from water radical cations $H_2O^{\bullet+}$ and hydroxyl radicals •OH, previously known to exist at water interfaces.

mesoporous silica particle | solid–water interface | cysteine oxidation | silyloxy radical | water radical cation

Significance

Considering the widespread use of mesoporous silica particles in our daily life as well as in medicine, the significant extent of oxidation facilitated by such previously considered chemically inert materials deserves much attention. Oxidation by such particles was studied in detail using nanoelectrospray ionization mass spectrometry. Data showed that more oxidation was measured when molecules have easier access to particle surfaces. Silyloxy radicals on particle surfaces are proposed to facilitate oxidation, and density functional theory calculations identified two possible pathways of the generation of such radicals at surfaces upon contact with water.

Silicon dioxide is a common food additive that acts as an anticaking agent, approved by the United States Food and Drug Administration (FDA). It is also regulated by the European Union (EU) under Regulation (EC, the European Parliament and of the Council) No 1333/2008; yet, the EU specification for silicon dioxide (E551) needs revision, according to the European Food Safety Authority, because it does not adequately characterize this substance in its use as a food additive (1). Apart from its use as an anticaking agent, silicon dioxide has many other potential applications in the food industry (2, 3). However, some health concerns have been raised about nanostructured synthetic amorphous silica, which requires further investigation (4). Synthetic amorphous silica and its derivatives are also widely used and deemed safe in cosmetics, based on final reports of the cosmetic ingredient review expert panel (5).

Furthermore, silica-based particles hold a strong potential in nanomedicine for clinical applications to benefit the society. For example, the first clinical trial of nanoparticle-based cancer-targeted imaging used these particles (6). Among such particles, mesoporous silica particles have high surface areas that allow them to carry a large amount of therapeutic drugs or imaging agents. They also have tunable pore structures that can control the release of chemicals. These particles are often regarded as biocompatible and nontoxic, making them suitable for medical applications. Additionally, they have been studied in vivo in mice for anticancer drug delivery systems (7). These particles have been found to accumulate in liver and other organs following injections, yet sometimes their biocompatibility is assumed simply based on the unchanged pathological sections of the liver in mice. Pure silica, also known as silicon dioxide, is generally recognized as a robust and safe inorganic material. Therefore, such a biomedical platform has been claimed to have a promising outlook for FDA approval (8).

Here, we present a straightforward chemical study showing that silica particles significantly facilitate oxidation of thiol-containing molecules, challenging the previous assumption of the chemical inertness of pure silica. Thiol-containing biomolecules, which are widespread in nature, play a crucial role in biological processes by forming disulfide bonds between cysteine residues to stabilize protein structures and are also essential for redox balance by reducing reactive oxygen species in the body (9). Oxidation of cysteine to disulfides happens as a prominent example of oxidative posttranslational modifications which play key roles in cell signaling and protein function, (10) and several probes have been developed to study such cysteine oxidation chemistry (11). Among thiol-containing biomolecules, glutathione plays a critical role in liver detoxification, but its oxidation can cause high levels of oxidative stress, leading to diseases and aging (12). Moreover, synthetic

Author affiliations: [a]Department of Chemistry, Stanford University, Stanford, CA 94305; and [b]Department of Chemistry, West Chester University, West Chester, PA 19383

Author contributions: Y.L. designed research; Y.L. and K.W.K. performed research; Y.L. and K.W.K. analyzed data; and Y.L., K.W.K., and R.N.Z. wrote the paper.

The authors declare no competing interest.

This article is a PNAS Direct Submission.

[1]To whom correspondence may be addressed. Email: lyj@stanford.edu or zare@stanford.edu.

This article contains supporting information online at https://www.pnas.org/lookup/suppl/doi:10.1073/pnas.2304735120/-/DCSupplemental.

Published August 17, 2023.

thiols, such as D-penicillamine, can be used as thiol-containing drugs to treat diseases (13). Therefore, the newly found reactivity of pure silica particles to facilitate thiol oxidation provides a molecular explanation for their reported toxicity (14). Recently, reactivity of a Menshutkin S_N2 reaction was reported to be enhanced by approximately twofold at solution/silica interfaces in mesoporous silica compared to bulk (15). Here, we report a much larger effects of porous silica on oxidation of thiols. We encourage further assessments on how key compounds such as glutathione could be depleted in one's body upon exposure to silica.

Results and Discussion

In this study, we tested the reactivity of silica by simply incubating solutions containing small molecules that have sulfhydryl (-SH) groups with pure silica particles whose purity was reported to be >99.99% by the vendor. The first model compound chosen in the study was glutathione because its redox couple (oxidized form glutathione disulfide represented by GSSG; reduced form glutathione represented by GSH) is abundant in cells and the ratio is known to serve as an important indicator of oxidative stress in a redox environment (16). Although the concentration of glutathione in plasma is often in few micromolar range, these extracellular pools are considered the key in detoxification against oxidants (17). Based on such consideration, 50 μM aqueous glutathione was analyzed after incubation with pure silica particles for certain periods of time. We used nanoelectrospray ionization mass spectrometry (nESI-MS) to analyze the signals of different species in reaction mixtures under the previously reported robust conditions for kinetic measurements (18–20).

Kinetic measurements of glutathione were performed from the supernatants of solutions incubated either with or without particles after centrifuging tubes at *ca.* 0.5 h (hour), 2 h, and 4 h, and the average measured values from three replicate experiments are plotted in Fig. 1. The peak ratios of oxidized glutathione ($[GSSG-2H]^{2-}$ at *m/z* 305.07) versus reduced glutathione ($[GSH-H]^-$ at *m/z* 306.08) were used to estimate the level of oxidative stress induced by these silica particles. The right panel of Fig. 1 shows the comparison of mass spectra collected under different conditions at 4 h. It is obvious from Fig. 1 that incubation with silica particles resulted in a greater amount of oxidation than that observed in control solutions without incubating with particles. While the control in blue showed 0.014 ± 0.002 in terms of the ratio of oxidized versus reduced glutathione signal at *m/z* 305.07 versus *m/z* 306.08 after 4 h, experiments with nonporous silica particles of 500-nm diameter in yellow showed a much larger ratio of 0.15 ± 0.02 after 4 h. We also found that the use of porous silica particles resulted in an even higher level of oxidation at a signal ratio of 0.29 ± 0.04 compared to the nonporous particles, which is attributed to their increased surface area. The signal ratios are plotted on the left panel of Fig. 1 to show the trend over time. Obviously, the extent of oxidation is found to increase over time, suggesting that the incubation with particles is the key factor leading to the much-increased oxidation.

In light of the findings on glutathione, we then tested how other thiol compounds including the amino acid L-cysteine and the thiol drug D-penicillamine can be affected by silica particles. In this experiment, we incubated different compounds with different particles and measured how much disulfide bond formations progress after 24 h. For different compounds, calibration curves using mixtures of the oxidized and reduced standards were studied to give a measure of ionization efficiency ratios for all three redox couples. After correcting for ionization efficiency ratios, oxidation yields were calculated based on the measured oxidized and reduced signals in mass spectra. Unlike the tripeptide glutathione whose disulfides tend to exist as doubly charged molecules in nESI-MS, oxidized species of cysteine and penicillamine tend to exist as singly charged molecules $[M-H]^-$, and thus, the signals of *m/z* at 239.02 and 120.01 were used for cysteine and signals of *m/z* at 295.08 and 148.04 were used for penicillamine. Oxidation yields were then plotted in Fig. 2 to compare different results between glutathione (in red), D-penicillamine (in blue), and L-cysteine (in green) under different conditions, with porous silica particles, with nonporous silica particles of 500-nm diameter, with nonporous silica particles of 3-μm diameter, and without any particles.

Based on the data in Fig. 2, we found that for all three low-molecular-weight thiols studied, incubation with porous silica particles and submicron-sized nonporous silica particles resulted in a greater amount of oxidation than that observed in control solutions incubated without particles. Yet, when using micron-sized nonporous silica particles, the level of oxidation was not as high as when using the other two particles studied. After the 1-d (1-day or 24-h) incubation with 500-nm nonporous silica particles, the yields of

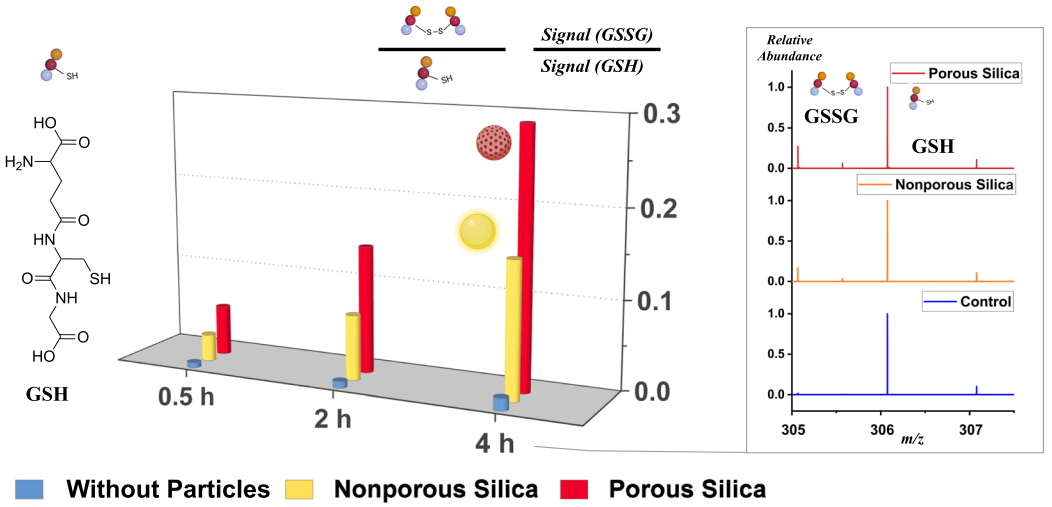

Fig. 1. The panel on the left shows kinetic measurements of glutathione oxidation via disulfide bond formation, showing significant increase in oxidation, measured by signals of oxidized species versus reduced species in mass spectra, after incubating with silica particles in water in dark. The panel on the right shows the mass spectra comparison measuring oxidized glutathione (GSSG) as well as the reduced species (GSH) under different conditions, (*Top*) incubated with mesoporous silica particles, (*Middle*) incubated with nonporous silica particles—500 nm in diameter, and (*Bottom*) without incubation with particles.

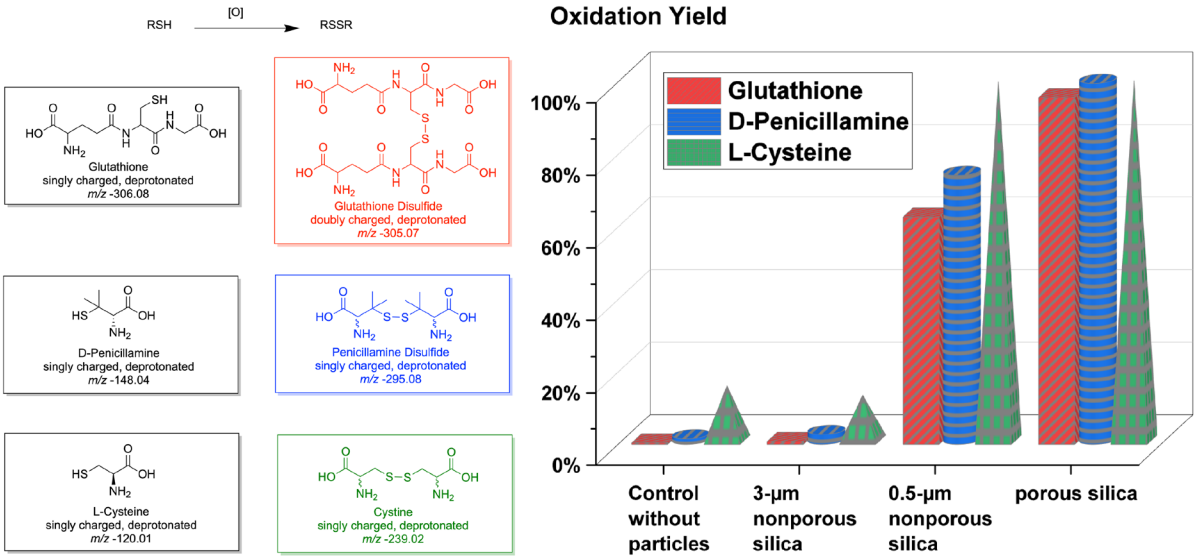

Fig. 2. Comparison of oxidation yields after 1-d incubation in dark of different reduced molecules (glutathione, D-penicillamine, and L-cysteine) with and without different particles (mesoporous silica particles, 500-nm nonporous silica, and 3-μm nonporous silica), after correction of ionization efficiency ratios for each set of chemicals.

oxidation for glutathione, penicillamine, and cysteine were 63%, 74%, and 99%, respectively. More surprisingly, for porous silica particles, almost full oxidation (>95% yield) was achieved for all three compounds. For glutathione after 24 h, the enhancement in oxidation yield was a factor of 233 for porous silica particles compared to the control. The data showed that the interaction between molecules with silica surfaces plays a vital role in the thiol oxidation process.

Reactions with thiols may vary with pH and the presence of peroxide, (21) but such causes are less likely in the case of induced disulfide bond formation by silica particles based on the following two relevant experiments we carried out. One phenomenon is that unlike soda lime glass microspheres, which were used as heterogeneous base catalysts, (22, 23) silica particles did not show the same effects to accelerate base-catalyzed Katritzky reactions. The second phenomenon is that hydrogen peroxide H_2O_2 was not measurable using the test paper (Quantofix peroxide 25 strips whose detection limit is 15 μM) and pH was measured to be unchanged (using the micro essential ultrafine pH paper) for the supernatant from ultrapure water or the studied aqueous solutions incubating with silica particles. Although in a different experimental setup hydrogen peroxide was generated by contact electrification which we are also actively pursuing further study on, (24) it does not seem applicable in the case here and is out of the scope of this current study due to lack of detectable hydrogen peroxide from the study of water incubating with pure silica particles. Also, although hydrogen peroxide H_2O_2 is known to form from stress-activated electric currents in rock as well as at the silica/water interface of freshly fractured surfaces of abraded quartz, we did not introduce any intensive mechanical forces into the system and thus we do not observe the stress-induced or fracture-induced formation of hydrogen peroxide (25, 26).

Also, sulfenic acid is a known intermediate when peroxide is present to cause oxidation of thiols (RSH representing thiol-containing compounds), (21) which was expected to show a $[RSOH\text{-}H]^-$ peak with a mass shift of +16 Th, but such a peak was not detected in high-resolution mass spectra throughout the kinetic processes measured. Dissolved molecular oxygen is known to be involved in the formation of disulfides as well, so we studied the oxidation of glutathione in detail using degassed water treated with freeze–pump–thaw cycles instead of using ultrapure water as received. These experiments as well as controls were also performed in triplicate (just as all the mass spectrometric experiments described above), as shown in Fig. 3. After 24 h, the average oxidation yield was 0.25% for 3-μm nonporous silica with surface areas measured to be 0.95 m^2/g by N_2 adsorption, which is 1.1-fold compared to the control without particles. For 500-nm nonporous silica with surface areas measured to be 3.6 m^2/g, the oxidation yield decreased significantly compared to previous experiments without degassing treatments, leading in a mild increase (2.9-fold) compared to the control and a small oxidation yield of 0.65%. This indicates that for nonporous silica, the exterior surfaces are good at trapping molecular oxygen to facilitate thiol oxidation, largely contributing to the 63% of glutathione oxidation seen previously without degassing the water. Yet, even after this rigorous degassing treatment, the enhancement in oxidation yield was a factor of 229 for porous silica particles compared to the control. Surface areas of such mesoporous silica particles were measured to be 650 m^2/g and the average oxidation yield after 24-h incubation was 51%. This acceleration factor was not too different from the factor of 233 when using the untreated ultrapure water, indicating that the silica surface itself contributes largely to the enhanced oxidation yields seen in mesoporous silica. We also attempted to test the light and dose response in such experiments, as shown in the right panel of Fig. 3. No light response was found using these particles compared to the experiments in dark, and larger extents of oxidation were found when more particles were used.

The lack of measurable hydrogen peroxide by the test paper or the lack of detectable relevant intermediates in the solution by mass spectrometry showed the specificity of silica-facilitated disulfide bond formation, which was also supported by our calculated results as shown in supporting information. Therefore, we propose that the silyloxy radical (SiO•) generated after the reaction of water with the particle's surface is what promotes thiol oxidation (step 1 in Fig. 4), and we explored the possibility of surface radical–initiated hydrogen abstraction to make a thiyl radical (RS•) for further combination into disulfides which is known to be rapid (27). Once such SiO• is generated on the silica surface, a thiol molecule after the initial physisorption (step 2 in Fig. 4) will transfer one H atom to the surface (step 3 in Fig. 4) while undergoing disulfide bond formation with a second thiol molecule in a further reaction step (step 4 and 5 in Fig. 4).

To achieve a deeper understanding of how these molecules interact with surfaces of silica, quantum chemical calculations

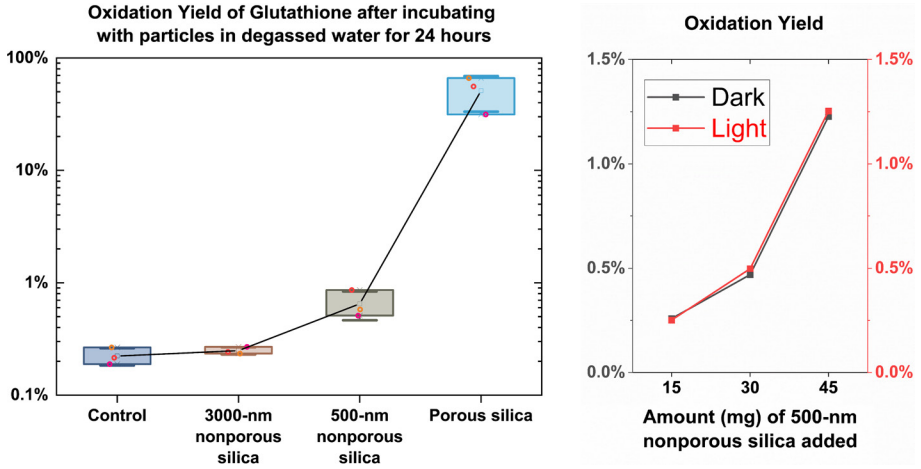

Fig. 3. The panel on the left shows comparison of oxidation yield after 1-d incubation in dark of glutathione in freeze–pump–thaw degassed water with and without particles (mesoporous silica particles, 500-nm nonporous silica, and 3-μm nonporous silica), after removal of dissolved gasses and correction of ionization efficiency ratios for reduced and oxidized glutathione. The right panel shows the dose dependence while no light response after 1-d incubation in freeze–pump–thaw degassed water.

were performed for reactions of molecules with silica surfaces derived from the α-quartz structure. Molecules such as cysteine and glutathione were first absorbed onto the silica surfaces by hydrogen bonding with terminal silanol groups, Si-OH, through -SH, -OH, and -NH- groups. Cysteine showed a binding energy of *ca.* 70 kJ/mol, whereas glutathione showed a stronger binding, 85 ± 17 and 106 ± 32 kJ/mol for the two different silica crystallographic planes studied, presumably from more hydrogen binding sites within the structure. These results are in accordance with the experimental observations of larger enhancement in oxidation for glutathione than cysteine after incubating with 500-nm nonporous silica particles compared to the control.

Total energy changes were calculated to show the formation of silyloxy radical on two different silica surfaces using density functional theory with a 6-31G* basis set, which was deemed sufficient for screening reactions, in combination with the ωB97X-D exchange-correlation functional. Consistent with the accepted pK_a of silica of 7, (28) deprotonation is found to be somewhat endothermic (*ca.* 75 kJ mol^{-1} or less). Direct formation of a surface-bound SiO• radical by H• removal is highly endothermic (>500 kJ mol^{-1}) and unlikely to occur spontaneously. Therefore, in our calculations, we searched for possible alternatives by screening reactions of silica surfaces with aqueous species previously known to exist including hydronium ion H^+, hydroxide ion OH^-, water radical cation $H_2O•^+$, (29) water radical anion $H_2O•^-$, hydrogen radical H•, hydroxyl radical •OH, (30) and bulk water H_2O, using clusters containing 0 to 25 water molecules.

Longer-lived partially charge water molecules ($H_2O^{+\delta}$ and $H_2O^{-\delta}$ with $\delta \approx 0.02$), formed via fleeting charge transfer in bulk water, are known to be in equilibrium with the water radical cation $H_2O•^+$ and a hydrated electron (the water radical anion $H_2O•^-$) (31). Although the partially charged water molecules may be long-lived, the latter radical cations are known to be short-lived, and the lifetime of such cation is known to be within <100 fs using femtosecond soft X-ray pulses as well as molecular dynamics simulations (32). Such a short-lived water radical cation, more often existing in its dimer form, (33, 34) can rapidly undergo proton transfer to form protonated hydroxyl radical (35, 36). In competition with proton transfer, situations where water radical cation $H_2O•^+$ undergoes electron transfer have also been studied. A transient absorption technique was used to time resolve reactivity of $H_2O•^+$ to oxidize species M into $M•^+$ in picosecond electron pulse radiolysis while the possibility of oxidation caused by •OH radicals was excluded in this case because it can only take place at a longer time (on the microsecond to nanosecond time scale). Also, evidence of water radical cation $H_2O•^+$ has been found when •OH

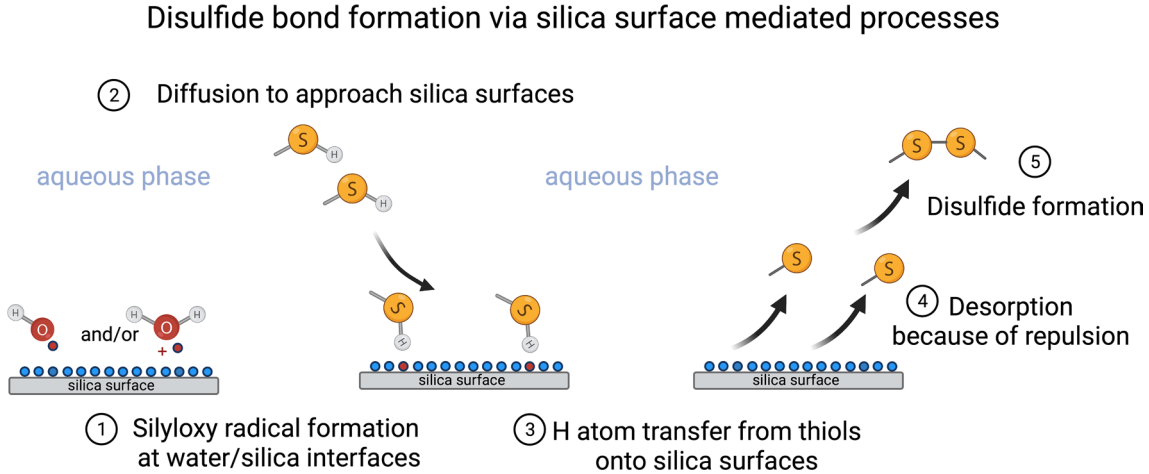

Fig. 4. A scheme shows proposed steps of molecule-surface interaction for the mechanism of thiol oxidation into disulfides without effects from dissolved gas. Red dots represent radicals while blue dots represent functional groups, silanols, at silica surfaces.

radicals can only provide certain but not all oxidized products observed, in the case of a guanine cation (37).

Recently, mass spectrometric experiments and computational results confirm the existence of both forms of the water radical dimer, the hydronium hydroxyl radical complex as well as the water bonded water radical cation complex. High-resolution mass spectrum measured water radical dimer at *m/z* 36.0207, and the tandem mass spectra of precursor ion *m/z* 36 gave both product ions at *m/z* 18 (formation of water radical cation after losing the neutral water molecule) and at *m/z* 19 (formation of hydronium after losing the neutral hydroxyl radical) (38). Also, water dimer radical cation generated from discharging water vapor showed two different characteristic reactivities. In the case to oxidize aromatic rings, it showed the characteristic of adding •OH radicals onto the compounds, reacting with a compound by H abstraction or addition (38, 39). While in the case of reacting with double bonds or with dimethyl disulfides, it showed characteristics of $H_2O^{\bullet+}$ (via one-electron transfer mechanism) in addition to protonated •OH radicals where both neutral loss of *m/z* 18 and *m/z* 17 were observed (29, 38).

Among all calculations we performed using 25 water molecules cluster, some key reactions are highlighted in *SI Appendix*, Table S3 where we show two much more plausible pathways of lowest energy to generate SiO• radicals from water radical cations (combined reaction #42 and #48) and •OH radicals (reaction #47), previously observed at water interfaces. This mechanism differs from what was proposed in the stress-induced or fracture-induced generation of hydrogen peroxide (26). Also, Reaction #23 and #48 shows the important role that $H_2O^{\bullet+}$ could play in the formation of both solution-phase •OH and surface-bound SiO• radicals. Although solution-phase •OH may well be generated from the $H_2O^{\bullet+}$ precursor, it is also possible that it is generated from OH^- at the high electric field at interfaces (24, 40). Also, one important factor to consider for the oxidative power of $H_2O^{\bullet+}$ is that the oxidation of molecules by $H_2O^{\bullet+}$ must be in situ. Otherwise, before the diffusion of $H_2O^{\bullet+}$ from its immediate proximity with another water molecule to reach another reducing agent, it can undergo proton transfer to generate the protonated •OH radical. This radical can diffuse faster and act as the oxidation intermediate for other solutes before its decay. Note that although we are not at the stage of pursuing which one of the intermediates is more likely to be consistent with what occurs to produce SiO• radicals at surfaces, both of these pathways are shown to be the most likely among other routes we investigated, not only energetically favored but also in accordance to the existences of these species at interfaces where silica is in immediate proximity to generate SiO• radicals.

All the experimental and calculation results lead us to propose the mechanism of how mesoporous silica oxidize thiols into disulfides, as shown in Fig. 4. In the first step, water radical cations or surface-bonded hydroxyl radicals initiate silyloxy radicals at silica surfaces once in contact with water. Thiol-containing molecules after being diffused to approach silica surfaces can form hydrogen bonding and physically adsorbed onto silica surfaces and undergo H atom transfer to form thiyl radicals, which can then be desorbed from the silica surface due to repulsion from the surface based on our calculations described in supporting information. Once thiyl radicals diffuse back into the aqueous phase, they can then recombine to form disulfide bonds.

Conclusions

In summary, our experimental results demonstrate that disulfide formation from thiol groups is enhanced dramatically, by up to two orders of magnitude, by incubation with both mesoporous silica particles and nonporous silica particles of submicron sizes under the studied conditions. This unexpected phenomenon of increased oxidation of thiol compounds by pure silica serves as a warning considering the wide use of silica in food and cosmetic products as well as the significance of thiol compounds in biology. At the same time, further safety assessments are in urgent need prior to loading therapeutics into silica particles for nanomedicine. Nanoelectrospray mass spectrometry for analysis of the supernatant in this study provides a simple experimental procedure to further assess how biologically important molecules or therapeutics undergo chemical modification upon contact with silica or related particles in solution. Our simulations identify plausible pathways of how aqueous species such as hydroxyl radicals or water radical cations can play a role to generate silyloxy radicals on silica surfaces, even though they may not directly participate in altering thiol chemistry. After thiol compounds are physically absorbed on silica surfaces via hydrogen bonding, such surface-bound radicals can abstract hydrogen from thiols to make thiyl radicals which further recombine to form disulfide bonds. Both disulfides and unreacted thiols then diffuse back into solution phase and could then be detected by mass spectrometric analysis.

Materials and Methods

Materials. Reduced molecules with free thiol groups were dissolved in water and then incubated with commercially available silica particles in the dark under ambient conditions (room temperature and atmospheric pressure). Such compounds, L-cysteine (lot #BCCF7968, TraceCERT®: 99.4% ± 0.3% purity), glutathione (lot #LRAC4116, 98.7% ± 0.7% purity), and D-penicillamine (lot #STBK2762, ≥98%), were purchased from Millipore Sigma. American Society for Testing and Materials (ASTM international standard) type I ultrapure water was purchased from Ricca Chemical (Natural poly bottle, catalog #9150 from Fisher Scientific). Water was used as received unless otherwise noted (treated with freeze–pump–thaw cycles in such experiments for Fig. 3). Monodisperse silica particles used, ranging from nanometers to microns, were uniform in size and pore size (if they are porous), reported by the vendor, Glantreo (Ireland), and the purity of silica was reported to be larger than 99.99% with impurity of Na (<40 ppm), K (<20 ppm), and Cl (<0.25 ppm). Porous silica particles used were the SOLAS™ powder, # PFPP0.50100R-5. Nonporous silica particles used were the SOLAD™ powder, # PNPP0.50NAR-5 as well as # PNPP3.0NAR-5.

Characterization of Silica. More details are described in *SI Appendix*.

Reactions. Each silica sample of 15 mg was weighed in an Eppendorf safe-lock plastic tube (polypropylene) and then 450 μL of the freshly prepared aqueous solution containing 50 μM of reduced molecules was added to incubate with the silica powder and thoroughly mixed immediately afterward. Then, the tubes, shut tightly and used as reaction containers, were allowed to sit undisturbed at room temperature, organized in vial racks. In the kinetic measurements, after a certain desired time, i.e., *ca.* 0.5 h, 2 h, 4 h, sampling of 10 μL aliquots was performed after centrifuging the tube for 10 min to allow sampling of supernatant from the reaction mixture. And after the sampling, the particles were redispersed using the vortex mixer to allow further kinetic measurements from the same reaction. Control experiments were performed three times by incubating the solution without particles under the same conditions. In the latter experiments, ultrafiltration devices were used at the end of the incubation to filter particles out, and the filtrate was used for further analysis from the liquid. In such an experiment, an Amicon Ultra-0.5 Centrifugal filter unit with Ultracel-100 regenerated cellulose membrane was used (of 100-kDa molecular weight cut off). Right before the use of the unit, ultrapure water was used to rinse the membrane as instructed, and then, the solution with particles was transferred into the unit. Particles were filtered out on top of the membrane following a 10-min spinning in a centrifuge, and the filtrate can then be used for the analysis of reaction progress. In these experiments, the oxidation yield was calculated from signal ratios in mass spectra after correcting for ionization efficiency ratios measured after making the three calibration curves for the mixtures of each reduced and oxidized compound. Oxidized compounds, L-cystine (lot #BCCD1578, TraceCERT®: 98.9% ±

0.8% purity), oxidized glutathione (lot #SLBS5804, ≥98%), and D-penicillamine disulfide (lot #MKCM2360, 97%), were also purchased from Millipore Sigma. Three replicates of experiments and controls were conducted in parallel, and the average value was used to show in the figures.

Analysis. The measurement of oxidative stress was carried out using nano-electrospray ionization mass spectrometry on either the supernatant or filtrate. Thin-wall borosilicate glass without filament was purchased from Sutter Instruments, cleaned by sonication in a mixed solvent, acetone: methanol: isopropanol = 1:1:2, and let air-dried. The capillaries were pulled into nano-electrospray emitters with ca. 2-μm tip inner diameter using a Flaming/Brown micropipette puller (P-87 by Sutter Instruments). An electrode made of 304 stainless steel wire (0.25 mm in diameter; 0.14464 Ω/cm reported by Scientific Instrument Services) was mounted in an electrode holder (Warner Instruments) and a short distance of *ca.* 3 mm was kept between the sprayer tip and a mass spectrometer inlet for nanoelectrospray ionization mass spectrometry. The mass spectrometer used for mass analysis was an Orbitrap instrument (ThermoFisher Orbitrap Velos Pro hybrid instrument). The source parameters used were mass spectrometer capillary temperature at 300 °C, source voltage at +1.5 kV applied on the nanoelectrospray electrode by a clip, S-lens RF (radio frequency) level at 20 (optimized to maximize signals for the chosen compounds). Mass spectra were recorded in a mass range from 100 to 350 and an average of 20 scans of FTMS spectra at a resolution of 480,000 was used in each trial. Monoisotopic peak height ratios were used for calculating signal ratios for oxidized and reduced species.

Computations. More details are described in *SI Appendix*.

Data, Materials, and Software Availability. All study data are included in the article and/or *SI Appendix*.

ACKNOWLEDGMENTS. Y.L. and R.N.Z. acknowledge the support from the Air Force Office of Scientific Research through the Multidisciplinary University Research Initiative program (AFOSR FA9550-21-1-0170). K.W.K. acknowledges the support from the NSF MRI program under award number 2216272. We acknowledge Daniel P. Marron from Prof. Robert M. Waymouth's lab for assistance in preparing freeze–pump–thaw degassed water. We acknowledge Samantha Shumlas, Director of the WCU (West Chester University) Center for Microanalysis and Imaging Research and Training (CMIRT) for scanning electron microscopy (SEM) imaging as well as Abbie Ganas and Zachary Voras for assistance with porosimetry and X-ray fluorescence (XRF) measurements, respectively. Fig. 4 and parts of Fig. 1 were created with BioRender.com.

1. EFSA Panel on Food Additives and Nutrient Sources added to Food (ANS) *et al.*, Re-evaluation of silicon dioxide (E 551) as a food additive. *EFSA J.* **16**, e05088 (2018).
2. M. R. Kasaai, Nanosized particles of silica and its derivatives for applications in various branches of food and nutrition sectors. *J. Nanotechnol.* **2015**, e852394 (2015).
3. D. Videira-Quintela, O. Martin, G. Montalvo, Emerging opportunities of silica-based materials within the food industry. *Microchem. J.* **167**, 106318 (2021).
4. H. C. Winkler, M. Suter, H. Naegeli, Critical review of the safety assessment of nano-structured silica additives in food. *J. Nanobiotechnol.* **14**, 44 (2016).
5. L. C. Becker *et al.*, Safety assessment of silylates and surface-modified siloxysilicates. *Int. J. Toxicol.* **32**, 5S–24S (2013).
6. E. Phillips *et al.*, Clinical translation of an ultrasmall inorganic optical-PET imaging nanoparticle probe. *Sci. Transl. Med.* **6**, 260ra149 (2014).
7. Z. Li, J. C. Barnes, A. Bosoy, J. F. Stoddart, J. I. Zink, Mesoporous silica nanoparticles in biomedical applications. *Chem. Soc. Rev.* **41**, 2590 (2012).
8. J. G. Croissant, Y. Fatieiev, A. Almalik, N. M. Khashab, Mesoporous silica and organosilica nanoparticles: Physical chemistry, biosafety, delivery strategies, and biomedical applications. *Adv. Healthcare Mater.* **7**, 1700831 (2018).
9. K. Ulrich, U. Jakob, The role of thiols in antioxidant systems. *Free Radic. Biol. Med.* **140**, 14–27 (2019).
10. L. Schulte *et al.*, Cysteine oxidation and disulfide formation in the ribosomal exit tunnel. *Nat. Commun.* **11**, 5569 (2020).
11. L. J. Alcock, M. V. Perkins, J. M. Chalker, Chemical methods for mapping cysteine oxidation. *Chem. Soc. Rev.* **47**, 231–268 (2018).
12. L. D. DeLeve, N. Kaplowitz, Glutathione metabolism and its role in hepatotoxicity. *Pharmacol. Ther.* **52**, 287–305 (1991).
13. A. R. Pfaff, J. Beltz, E. King, N. Ercal, Medicinal thiols: Current status and new perspectives. *Mini Rev. Med. Chem.* **20**, 513–529 (2020).
14. S. E. Lehman *et al.*, Silica nanoparticle-generated ROS as a predictor of cellular toxicity: Mechanistic insights and safety by design. *Environ. Sci. Nano* **3**, 56–66 (2016).
15. W. Zheng *et al.*, Enhanced menshutkin SN2 reactivity in mesoporous silica: The influence of surface catalysis and confinement. *J. Am. Chem. Soc.* **142**, 5636–5648 (2020).
16. F. Q. Schafer, G. R. Buettner, Redox environment of the cell as viewed through the redox state of the glutathione disulfide/glutathione couple. *Free Radic. Biol. Med.* **30**, 1191–1212 (2001).
17. C. V. Smith, D. P. Jones, T. M. Guenthner, L. H. Lash, B. H. Lauterburg, Compartmentation of glutathione: Implications for the study of toxicity and disease. *Toxicol. Appl. Pharmacol.* **140**, 1–12 (1996).
18. Y. Li *et al.*, Accelerated forced degradation of pharmaceuticals in levitated microdroplet reactors. *Chem. Eur. J.* **24**, 7349–7353 (2018).
19. Y. Li *et al.*, Accelerated forced degradation of therapeutic peptides in levitated microdroplets. *Pharm. Res.* **37**, 138 (2020).
20. Y. Li, T. F. Mehari, Z. Wei, Y. Liu, R. G. Cooks, Reaction acceleration at air-solution interfaces: Anisotropic rate constants for Katritzky transamination. *J. Mass Spectr.* **56**, e4585 (2021).
21. L. Grassi, C. Cabrele, Susceptibility of protein therapeutics to spontaneous chemical modifications by oxidation, cyclization, and elimination reactions. *Amino Acids* **51**, 1409–1431 (2019).
22. Y. Li, T. F. Mehari, Z. Wei, Y. Liu, R. G. Cooks, Reaction acceleration at solid/solution interfaces: Katritzky reaction catalyzed by glass particles. *Angew. Chem. Int. Ed.* **60**, 2929–2933 (2021).
23. Y. Li, K.-H. Huang, N. M. Morato, R. Graham Cooks, Glass surface as strong base, 'green' heterogeneous catalyst and degradation reagent. *Chem. Sci.* **12**, 9816–9822 (2021).
24. B. Chen *et al.*, Water–solid contact electrification causes hydrogen peroxide production from hydroxyl radical recombination in sprayed microdroplets. *Proc. Natl. Acad. Sci. U.S.A.* **119**, e2209056119 (2022).
25. M. Balk *et al.*, Oxidation of water to hydrogen peroxide at the rock–water interface due to stress-activated electric currents in rocks. *Earth Planet. Sci. Lett.* **283**, 87–92 (2009).
26. H. He *et al.*, A mineral-based origin of Earth's initial hydrogen peroxide and molecular oxygen. *Proc. Natl. Acad. Sci. U.S.A.* **120**, e2221984120 (2023).
27. P. Wardman, C. von Sonntag, "[3] Kinetic factors that control the fate of thiyl radicals in cells" in *Methods in Enzymology, Biothiols Part A Monothiols and Dithiols, Protein Thiols, and Thiyl Radicals*, (Academic Press, 1995), pp. 31–45.
28. S. H. Behrens, D. G. Grier, The charge of glass and silica surfaces. *J. Chem. Phys.* **115**, 6716–6721 (2001).
29. L. Qiu, N. M. Morato, K.-H. Huang, R. G. Cooks, Spontaneous water radical cation oxidation at double bonds in microdroplets. *Front Chem.* **10**, 903774 (2022).
30. J. K. Lee, D. Samanta, H. G. Nam, R. N. Zare, Micrometer-sized water droplets induce spontaneous reduction. *J. Am. Chem. Soc.* **141**, 10585–10589 (2019).
31. D. Ben-Amotz, Electric buzz in a glass of pure water. *Science* **376**, 800–801 (2022).
32. Z.-H. Loh *et al.*, Observation of the fastest chemical processes in the radiolysis of water. *Science* **367**, 179–182 (2020).
33. P. A. Pieniazek, J. VandeVondele, P. Jungwirth, A. I. Krylov, S. E. Bradforth, Electronic structure of the water dimer cation. *J. Phys. Chem. A* **112**, 6159–6170 (2008).
34. Q. Cheng, F. A. Evangelista, A. C. Simmonett, Y. Yamaguchi, H. F. I. Schaefer, Water dimer radical cation: Structures, vibrational frequencies, and energetics. *J. Phys. Chem. A* **113**, 13779–13789 (2009).
35. M.-F. Lin *et al.*, Imaging the short-lived hydroxyl-hydronium pair in ionized liquid water. *Science* **374**, 92–95 (2021).
36. Y. Gauduel, S. Pommeret, A. Migus, A. Antonetti, Some evidence of ultrafast H_2O^+-water molecule reaction in femtosecond photoionization of pure liquid water: Influence on geminate pair recombination dynamics. *Chem. Phys.* **149**, 1–10 (1990).
37. J. Ma, F. Wang, M. Mostafavi, Ultrafast chemistry of water radical cation, $H_2O^{\bullet+}$, in aqueous solutions. *Molecules* **23**, 244 (2018).
38. M. Wang *et al.*, Abundant production of reactive water radical cations under ambient conditions. *CCS Chem.* **4**, 1224–1231 (2021).
39. D. Xing *et al.*, Capture of hydroxyl radicals by hydronium cations in water microdroplets. *Angewandte Chemie* **134**, e202207587 (2022).
40. H. Hao, I. Leven, T. Head-Gordon, Can electric fields drive chemistry for an aqueous microdroplet? *Nat. Commun.* **13**, 280 (2022).